Title

VEGF Inhibits Tumor Cell Invasion and Mesenchymal Transition through a MET/VEGFR2 Complex

Journal

Cancer Cell, 22(1)

ISSN

1535-6108

Authors

Lu, Kan V
Chang, Jeffrey P
Parachoniak, Christine A
et al.

Publication Date

2012-07-01

DOI

10.1016/j.ccr.2012.05.037

Peer reviewed

Published in final edited form as:
Cancer Cell. 2012 July 10; 22(1): 21–35. doi:10.1016/j.ccr.2012.05.037.

VEGF Inhibits Tumor Cell Invasion and Mesenchymal Transition Through a MET/VEGFR2 Complex

Kan V. Lu[1,3], **Jeffrey P. Chang**[1,3], **Christine A. Parachoniak**[5], **Melissa M. Pandika**[1,3], **Manish K. Aghi**[1,3,4], **David Meyronet**[1,3], **Nadezda Isachenko**[1,3], **Shaun D. Fouse**[1,3], **Joanna J. Phillips**[1,3,4], **David A. Cheresh**[6], **Morag Park**[5], and **Gabriele Bergers**[1,2,3,4,*]

[1]Departments of Neurological Surgery, University of California, Helen Diller Family Cancer Research Center, San Francisco, California 94143, USA

[2]Anatomy, University of California, Helen Diller Family Cancer Research Center, San Francisco, California 94143, USA

[3]Brain Tumor Research Center, University of California, Helen Diller Family Cancer Research Center, San Francisco, California 94143, USA

[4]UCSF Comprehensive Cancer Center, University of California, Helen Diller Family Cancer Research Center, San Francisco, California 94143, USA

[5]Department of Biochemistry and Goodman Cancer Research Centre, McGill University, Montreal, Quebec, Canada

[6]Department of Pathology and Moore's UCSD Cancer Center, University of California, San Diego, California 92093, USA

Summary

Inhibition of VEGF signaling leads to a pro-invasive phenotype in mouse models of glioblastoma multiforme (GBM) and in a subset of GBM patients treated with bevacizumab. Here we demonstrate that vascular endothelial growth factor (VEGF) directly and negatively regulates tumor cell invasion through enhanced recruitment of the protein tyrosine phosphatase 1B (PTP1B) to a MET/VEGFR2 heterocomplex, thereby suppressing HGF-dependent MET phosphorylation and tumor cell migration. Consequently, VEGF blockade restores and increases MET activity in GBM cells in a hypoxia-independent manner, while inducing a program reminiscent of epithelial-to-mesenchymal transition highlighted by a T-cadherin to N-cadherin switch and enhanced mesenchymal features. Inhibition of MET in GBM mouse models blocks mesenchymal transition and invasion provoked by VEGF ablation, resulting in substantial survival benefit.

[*]Correspondence should be addressed to: University of California, San Francisco (UCSF) Helen Diller Family Cancer Research Center Department of Neurological Surgery 1450 3rd Street San Francisco, California 94143, USA gabriele.bergers@ucsf.edu Telephone: 415-476-6786 Fax: 415-476-0388.

Introduction

Glioblastoma multiforme (GBM) are characterized by rapid and invasive growth throughout the brain. Despite standard and targeted therapies median overall survival of GBM patients remains just over one year (Furnari et al., 2007). GBM are also one of the most vascularized and edematous tumors as they express high levels of VEGF (Ferrara et al., 2003; Sundberg et al., 2001; van Bruggen et al., 1999). Encouragingly, bevacizumab, a humanized monoclonal antibody against VEGF, has demonstrated therapeutic benefit in many GBM patients when used alone or in combination with irinotecan (Friedman et al., 2009; Vredenburgh et al., 2007). This led to the accelerated approval of bevacizumab by the US Food and Drug Administration in 2009 for use as a single agent in recurrent GBM, and its use in the frontline setting for newly diagnosed GBM is currently being evaluated.

Despite initial responsiveness, however, the beneficial effects of bevacizumab are transient, and GBM inevitably progress during anti-VEGF treatment by adapting and utilizing alternative pathways to sustain tumor growth, all while VEGFR signaling remains inhibited (Bergers and Hanahan, 2008).

Clinical evidence suggests that GBM relapse during anti-VEGF therapy can present with at least two differing radiographic patterns representing distinct mechanisms of evasion. While most GBM patients develop characteristic local recurrences that regain the ability to induce neovascularization as observed by increased magnetic resonance imaging (MRI) contrast enhancement, up to 30% of GBM patients demonstrate a more extensive, infiltrative, and distant disease that lacks angiogenic induction and is non-contrast enhancing, but is instead detectable by fluid-attenuated inversion recovery (FLAIR) MRI (de Groot et al., 2010; Iwamoto et al., 2009; Rose and Aghi, 2010). While the incidence of invasion has been a subject of discussion due the current lack of a standardized definition for radiographic relapse (Chamberlain, 2011; Wick et al., 2011), the frequency of invasive non-enhancing tumors nevertheless appears to be higher than would be expected in patients who do not receive bevacizumab (Iwamoto et al., 2009). This pro-invasive recurrence encumbers surgical resection of recurrent GBM and challenges further therapeutic options for patients.

Similar to other studies using mouse models of GBM (de Groot et al., 2010; Kunkel et al., 2001; Rubenstein et al., 2000), we have observed that a more perivascular invasive phenotype, in which tumor cells move predominantly along blood vessels deep into the brain parenchyma, was induced when murine GBM were unable to initiate angiogenesis, a phenomenon that predicted the invasive relapse pattern seen in bevacizumab-treated human GBM (Blouw et al., 2003; Du et al., 2008a; Paez-Ribes et al., 2009). The enhanced invasiveness was a result of impairing tumor angiogenesis either through genetic ablation of key angiogenic factors that drive VEGF-dependent neovascularization (HIF-1α, VEGF, MMP-9, MMP-2) (Blouw et al., 2003; Du et al., 2008a; Du et al., 2008b) or by pharmacologic targeting of VEGF signaling (Paez-Ribes et al., 2009). We further revealed an unexpected link between HGF and VEGF, in which VEGF reduced the chemotactic activity of GBM cells towards HGF in vitro (Du et al., 2008a). The HGF receptor MET, a receptor tyrosine kinase that is frequently deregulated in many cancers and promotes proliferation, scattering, invasion, survival, and angiogenesis (Birchmeier et al., 2003; Rong

et al., 1992; Trusolino et al., 2010; Wang et al., 2001), is correlated with increased tumor invasion and poorer survival in GBM (Abounader and Laterra, 2005; Koochekpour et al., 1997; Lamszus et al., 1998).

Given that VEGF inhibition was a common denominator among the various genetic knockout models and pharmacologic treatments described above, we investigated whether VEGF itself might act as a regulatory switch for GBM invasion through regulating MET.

Results

Intratumoral VEGF Levels Inversely Correlate with MET Phosphorylation and Invasion of GBM Tumor Cells

To test our hypothesis that VEGF regulates the HGF/MET axis in tumor cells, we used orthotopically implanted SV40 large T-antigen and H-ras transformed mouse astrocytoma cell lines differing only in their VEGF expression levels: VEGFKO GBM, which are genetically ablated of VEGF expression; WT-GBM, which produce endogenous levels of VEGF; and VEGFKO-VEGF GBM, which are VEGFKO GBM cells expressing a high level of exogenous VEGF (Figures 1A and 1B). VEGFKO tumors were non-angiogenic and grew as extensively diffuse and invasive tumor cell clusters along normal blood vessels deep into the brain parenchyma (Figure 1A) (Blouw et al., 2003). In contrast, WT-GBM cells generated angiogenic tumors with locally infiltrative tumor cells characteristic of human GBM and VEGFKO-VEGF cells produced highly vascular, tightly packed tumors with smooth borders (Figure 1A). We then assessed whether changes in MET expression and activation could account for differences in invasive capacity. Immunohistochemical staining and western blot analysis of total MET in orthotopic murine GBM xenografts and cell lines showed abundant and similar MET expression regardless of VEGF expression levels (Figures 1C and S1A-C). In contrast, phospho-MET (P-MET) staining revealed strong positivity in invading clusters of VEGFKO GBM, marginal staining in a few invading tumor cells in WT-GBM, and no staining throughout VEGFKO-VEGF GBM (Figure 1D). These observations were recapitulated in another murine GBM model (NSCG) in which neural stem cells were isolated from the subventricular zone of Ink4a/Arf deficient mice and transduced with the constitutively active mutant receptor EGFRvIII (Phillips et al., 2012) (Figures S1D-F).

Importantly, when we assessed P-MET in GBM specimens from patients who had relapsed during bevacizumab therapy, we observed stronger and more abundant positivity in tumors post-treatment compared to matched pre-treated samples in 7 out of 10 patients (Figures 1E and 1F). These data indicate that loss of VEGF induces MET activation in invading tumor cells without necessarily increasing MET expression, and inferred a mechanism distinct from that of intratumoral hypoxia induced by anti-VEGF therapy causing transcription of hypoxia-regulated pro-invasive genes such as *Met* to perpetuate invasion.

VEGF Directly and Negatively Regulates GBM Invasion by Inhibiting MET Activation

We then asked whether VEGF could signal directly on tumor cells to affect MET activity and invasiveness. We first examined whether VEGF perturbed the HGF/MET signaling

pathway. To test this, VEGFKO cells were stimulated with HGF alone or in combination with VEGF. HGF treatment resulted in robust phosphorylation of MET and of FAK, which were decreased by VEGF in a dose-dependent manner (Figure 2A). Similarly, MET and FAK activation induced by HGF were reduced when VEGFKO cells were incubated with VEGFKO-VEGF conditioned medium (CM), but not VEGFKO CM (Figure 2A). Total MET expression was unaltered by VEGF. In contrast, stimulation with increasing concentrations of HGF in the presence of high VEGF levels dose-dependently restored P-MET and P-FAK, supporting an antagonistic and dynamic interplay between VEGF and HGF on MET signaling (Figure 2A). VEGF also inhibited P-MET and P-FAK in human GBM43 cells derived from a GBM patient (Sarkaria et al., 2006) (Figure 2B). The antagonistic interaction between VEGF and HGF/MET appeared specific, as neither EGF nor PDGF suppress P-MET or P-FAK induced by HGF (Figure S2A). Treatment of GBM43 cells with the function-blocking anti-VEGF monoclonal antibody B20 (Liang et al., 2006) abrogated P-MET suppression by VEGF (Figure 2C), further supporting a specific role for VEGF in regulating MET activation.

We next determined whether VEGF affected HGF-dependent GBM cell invasion by performing a wound-healing assay. HGF-treated VEGFKO cells closed nearly the entire wound area within 16 hours, while addition of exogenous VEGF significantly diminished their migration (Figure 2D). Similarly, VEGFKO-VEGF cells exhibited reduced migratory capacity, and application of VEGFKO-VEGF CM onto VEGFKO cells impeded cell migration (Figure 2D). Overexpression of VEGF or incubation with VEGFKO-VEGF CM also reduced P-MET in NSCG and GBM43 cells and hindered their migration (Figures S2B-C; Figure 2E). These studies demonstrate that VEGF directly impedes HGF-dependent MET signaling and migration in murine and human GBM cells.

VEGF Requires VEGFR2 to Inhibit MET Activation and Cell Motility

How does VEGF block HGF/MET signaling? One might envision that VEGF directly competes with HGF for MET binding or that VEGF antagonizes MET activity by signaling through VEGF receptors on tumor cells (Figure 3A). Congruent with reports that a variety of tumor cells express VEGF receptors (Lesslie et al., 2006; Spannuth et al., 2009; Wang et al., 2010), we found that murine and human GBM cells express VEGFR1 and VEGFR2 (Figures 3B, S3A and S3B) and that many tumor cell lines representing other cancer types for which bevacizumab has been approved, also express VEGF receptors at various levels (Figure S3C).

Using neutralizing antibodies against VEGFR1 (MF1) and VEGFR2 (DC101), we found that VEGF-dependent suppression of HGF-mediated P-MET and P-FAK in GBM cells was abrogated by addition of DC101, but not MF1 (Figure 3C). Congruently, while VEGFKO cells treated with VEGFKO-VEGF CM were significantly less motile, DC101 treatment restored their ability to migrate, whereas MF1 did not (Figure 3D). We then stably silenced VEGFR2 in VEGFKO cells by shRNA (Figure 3E). Whereas scrambled shRNA had no effect on the negative regulation of P-MET by VEGF, shVEGFR2 resulted in sustained P-MET in the presence of VEGF (Figure 3F). Finally, addition of VEGF to HEK293T fibroblasts, which lack VEGFR2 expression, failed to suppress HGF-stimulated P-MET or

P-FAK (Figures 3G and 3H), supporting the need for VEGFR2 and ruling out direct competition between HGF and VEGF for MET.

We then asked whether the VEGF co-receptor neuropilin-1 (NRP-1) is involved in mediating VEGF inhibition of P-MET. NRP-1 enhances signaling of the $VEGF_{165}$ isoform on VEGFR2 but is unable to bind the $VEGF_{121}$ isoform (Soker et al., 1998). VEGFKO cells stimulated with $VEGF_{121}$ were still able to diminish HGF-stimulated P-MET (Figure 3I), and NRP-1 did not co-precipitate with VEGFR2/MET (data not shown), indicating that the inhibitory effect of VEGF is independent of NRP-1.

Finally, given the negative regulation of VEGF on MET activation, we considered whether HGF could conversely affect VEGFR2 signaling. VEGF stimulation of GBM43 cells led to VEGFR2 phosphorylation and weak downstream activation of Akt and MAPK (Figure S3D), whereas HGF stimulation resulted in substantially more potent Akt and MAPK phosphorylation. Co-stimulation with HGF and VEGF did not perturb VEGFR2 phosphorylation (Figure S3D), suggesting that HGF/MET signaling does not negatively regulate VEGF/VEGFR2 signaling under these conditions.

Physical Association of MET and VEGFR2

We next evaluated whether VEGFR2 and MET physically associate with each other by performing reciprocal immunoprecipitation (IP) studies. IP of primary human GBM cells expressing detectable levels of MET and VEGFR2 with a VEGFR2 antibody followed by immunoblotting for MET revealed an physical interaction between these two endogenous proteins (Figure 4A). We then transduced VEGFKO and GBM43 cells with HA-tagged wild type (WT)-VEGFR2 or a truncated VEGFR2 mutant lacking the C-terminal 450 amino acids encompassing key kinase and effector domains (VEGFR2-Δ450C). IP of these cells with a MET antibody or a HA-Tag antibody revealed an interaction of MET with WT-VEGFR2 but not with VEGFR2-Δ450C (Figures 4B and 4C), indicating that the C-terminal region of VEGFR2 is required for MET association. The physical association between MET and VEGFR2 was observed independent of stimulation of either receptor with its cognate ligand, but P-MET co-precipitated only when cells were stimulated with HGF, and addition of VEGF suppressed HGF-stimulated P-MET only when cells were transduced with WT-VEGR2, not VEGFR2-Δ450C (Figure 4B).

Similar to the IP studies, proximity ligation assay (PLA) (Soderberg et al., 2008) demonstrated an interaction between MET and WT-VEGFR2, but not with VEGFR2-Δ450C, in VEGFKO and GBM43 cells irrespective of stimulation with either ligand (Figure 4D). However, when GBM cells expressing WT-VEGFR2 were co-stimulated with HGF and VEGF, the number of PLA spots per cell was slightly reduced but the size of these spots increased (Figures 4D-4G). These results suggest that additional proteins might associate with and redistribute the complex when both ligands are present.

VEGF Enhances Recruitment of the Tyrosine Phosphatase PTP1B to MET and Facilitates Downregulation of HGF-induced MET Phosphorylation

Several mechanisms for attenuation of MET signaling have been described, including internalization and degradation, as well as dephosphorylation by specific tyrosine

phosphatases (Abella et al., 2005; Hammond et al., 2003; Sangwan et al., 2008). We found that VEGF stimulation did not decrease total MET over time (Figures 2A, 2B, S4A-C) or enhance the phosphorylation of Ser985 of MET (data not shown), a negative regulatory site that suppresses MET tyrosine phosphorylation (Gandino et al., 1994). In contrast, treatment of GBM43 cells with the tyrosine phosphatase inhibitor sodium orthovanadate abrogated the suppressive effect of VEGF on P-MET (Figure 5A), indicating the involvement of a tyrosine phosphatase. Among the various tyrosine phosphatases known to modulate MET activity is the non-receptor protein tyrosine phosphatase 1B (PTP1B), which can directly dephosphorylate various RTKs including MET and VEGFR2 (Nakamura et al., 2008; Sangwan et al., 2008). Knockdown of PTP1B in GBM43 cells abolished downregulation of P-MET by VEGF (Figure 5A), supporting a role for PTP1B in VEGF-dependent suppression of P-MET. We then asked whether the extent of interaction between PTP1B and MET was modulated in the presence of VEGF. Co-IP studies revealed low levels of PTP1B/MET interaction in untreated and VEGF-stimulated cells (Figure 5B). As expected, PTP1B/MET association was elevated when cells were stimulated with HGF, and was further increased when cells were co-stimulated with HGF and VEGF (Figure 5B). These data indicate that VEGF enhances recruitment of PTP1B to MET and facilitates dephosphorylation of HGF-induced P-MET.

Upon HGF stimulation, MET enters the endocytic pathway and is either targeted for lysosomal degradation or recycled back to the cell surface (Abella et al., 2005; Hammond et al., 2003). We thus considered whether VEGF could enhance MET dephosphorylation by altering MET internalization and trafficking kinetics. To this end, we tracked MET co-localization with established endosomal markers indicative of different stages of trafficking (Stenmark, 2009). In serum-starved, unstimulated or VEGF-treated GBM43 cells, MET was predominantly localized to the plasma membrane while HGF stimulation caused MET internalization into EEA-1 positive endosomes (Figures 5C and 5D). Co-stimulation of GBM43 cells with VEGF and HGF provided a modest but not statistically significant increase in MET/EEA-1 co-localization (Figure 5D). Similar results were observed in VEGFKO cells (data not shown). We also studied co-localization of MET with GFP-fusion constructs of the early endosome markers Rab5 and Rab4, the late endosome marker Rab7, and the recycling endosome marker Rab11. Under the same stimulation conditions and timeframe that revealed optimal VEGF-induced suppression of P-MET, we found MET predominantly in early endosomes upon stimulation with HGF irrespective of VEGF (Figure S4D-E). These results reveal that VEGF enhances recruitment of PTP1B to the VEGFR2/MET complex to facilitate MET dephosphorylation, but does not alter endocytosis and trafficking.

MET Knockdown Blocks Invasiveness during VEGF Ablation and Prolongs Survival

If HGF/MET signaling is indeed a key mediator of GBM migration and invasion, MET inhibition should suppress tumor invasion provoked by VEGF ablation. Thus, we stably knocked down MET expression in VEGFKO cells using two independent shRNAs (VEGFKO-shMET1 and –shMET2) by 85% and 60%, respectively (Figure 6A). VEGFKO-shMET1 cells displayed significantly impaired in vitro motility (Figure 6B) and proliferation (Figure S5A). Most importantly, VEGFKO-shMET1 tumors growing intracranially in mice

were substantially less invasive and grew as a solid mass even at end-stage (Figures S5B and S5C) in contrast to the extensive perivascular invasive phenotype of time-matched VEGFKO parental and scrambled-shRNA tumors (Figures 6C and 6D). Both the total number of invading cell clusters and invasion distance were considerably lower in VEGFKO-shMET1 tumors compared to VEGFKO tumors (Figures 6E and S5D-F). VEGFKO-shMET1 tumors also displayed lower in vivo proliferation (Figure 6F) and reduced vascular density (Figure 6G) compared to VEGFKO, indicating the pleiotrophic effects of MET signaling. These effects led to a three-fold prolongation of survival compared to WT-GBM, surpassing the survival benefit observed in VEGFKO over WT-GBM (Figure 6H). Notably, because the silencing effect in VEGFKO-shMET2 was less effective, MET-positive tumor cells eventually emerged over time, leading to invasive progression (Figures S5A, S5H-J) and reduced survival benefit over control tumors (Figure S5G). These results underscore MET as a critical driver of GBM invasion and strongly encourage combined anti-VEGF and anti-MET therapy for GBM patients.

HGF/MET Signaling Induces an EMT-like Mesenchymal Phenotype in GBM

Knocking down MET in VEGFKO cells also changed their spindle-like, fibroblastic morphology towards one in which they clustered together into islands with minimal astrocytic processes (Figure 7A) reminiscent of epithelial cells undergoing a mesenchymal-to-epithelial transition (Kalluri and Weinberg, 2009; Thiery et al., 2009). Several recent studies have raised the notion that a mesenchymal gene expression signature is associated with poorer prognosis in GBM patients (Phillips et al., 2006; Tso et al., 2006; Verhaak et al., 2010). Therefore we speculated that VEGF inhibition, and hence MET activation in GBM, may induce or enhance a switch to a more mesenchymal and aggressive state, analogous to the classical epithelial-to-mesenchymal transition (EMT) described in epithelial cells. Indeed, we found that VEGFKO cells gradually upregulated the EMT markers Snail and N-cadherin, but suppressed T-cadherin over a 24-hour time course of HGF stimulation (Figure 7B). These effects were dependent on MET, as HGF-stimulated VEGFKO-shMET1 cells were unable to induce Snail and N-cadherin or downregulate T-cadherin (Figure 7B). Consistent with a report that T-cadherin promotes glioma cell growth arrest (Huang et al., 2003), T-cadherin expression was higher in less invasive and slower growing VEGFKO-shMET1 cells than in VEGFKO cells (Figure 7C). Upregulation of N-cadherin was not associated with suppression of E-cadherin as VEGFKO cells lack E-cadherin expression (data not shown). Importantly, when HGF-induced P-MET and P-FAK was tempered by VEGF in VEGFKO cells, N-cadherin was correspondingly suppressed (Figure 7D).

In vivo, N-cadherin staining was observed in the centers of VEGFKO tumors but was substantially stronger in invading cells at the tumor periphery in correlation with strong P-MET staining found only in invading cells (Figure 7E). Conversely, VEGFKO tumor centers were weakly positive for T-cadherin and the invading cells were negative (Figure 7E). VEGFKO-shMET1 tumors had smooth borders and were positive for T-cadherin, whereas N-cadherin was weak in the tumor center and absent at the rim (Figure 7E).

We next tested whether increased MET activation due to VEGF ablation could indeed induce a more mesenchymal and aggressive phenotype. We pharmacologically inhibited

VEGF and angiogenesis in orthotopic WT-GBM tumors with the anti-VEGF antibody B20, which imparted a significant survival benefit mirroring that observed in VEGFKO tumors (Figure S6A). As expected, treatment of WT-GBM-bearing mice with B20 increased cell invasion at the tumor periphery compared to control tumors (Figure 7F and S6B). These invading cells were strongly positive for P-MET and correspondingly exhibited upregulation of N-cadherin and downregulation of T-cadherin (Figure 7F). In contrast, P-MET staining in control WT-GBM tumors was restricted to only a few infiltrating cells at the tumor periphery, similar to their limited pattern of N-cadherin expression (Figure 7F). T-cadherin was strongly expressed in many cells but not uniformly positive, with the frequency of positive cells diminishing toward the tumor edge (Figure 7F). Overall, MET phosphorylation was associated with tumor cell invasion, increased N-cadherin, and decreased T-cadherin expression. Similar results were observed when mice bearing WT-GBM tumors were treated with the broad-spectrum RTK inhibitor sunitinib, which also targets the VEGF pathway (Figure S6C). These results indicate that MET activation induces a mesenchymal transformation in GBM underscored by a T- to N-cadherin switch distinct from the classical E- to N-cadherin switch.

Bevacizumab-Resistant Human GBM Exhibit Increased MET Activation and Expression of Mesenchymal Markers

To determine whether mesenchymal markers are elevated in correlation with increased P-MET-positive invasive cell clusters in GBM patients after bevacizumab treatment, we examined our paired pre- and post-bevacizumab treatment patient tumor specimens. Of 7 relapsed tumors showing increased P-MET staining after treatment (Figures 1E and 1F), 6 exhibited a corresponding increase in the extent and intensity of N-cadherin staining (Figure 8A). Of these 6 tumors, 5 showed upregulation of the mesenchymal marker vimentin with 3 of them further displaying higher levels of CD44, a mesenchymal stem cell marker associated with GBM (Tso et al., 2006) (Figures 8A and 8B). In total, 8/9 analyzed tumor pairs demonstrated an increase in vimentin after bevacizumab treatment, while 6/9 exhibited increased CD44 (Figures 8A and 8B). Expression of YKL-40, a marker for the mesenchymal subtype of GBMs (Phillips et al., 2006), was also upregulated after bevacizumab treatment in 3/5 tumor pairs examined (Figure 8C). The mean staining intensities for vimentin, CD44, and YKL-40 were significantly higher in bevacizumab-resistant tumors than in paired pre-treatment specimens (Figure 8C). These results suggest that human GBM treated with targeted VEGF therapy may progress by switching to a more mesenchymal phenotype involving upregulation of MET activity and expression of key mesenchymal genes and markers.

Discussion

VEGF has been thought to act predominantly on the vasculature, given that its receptors are prevalent in endothelial cells and that deletion of either VEGF or VEGFR2 results in early embryonic lethality due to impaired hematopoietic and endothelial cell development (Ferrara, 2001; Olsson et al., 2006). The main signaling circuit of VEGF is thought to be VEGFR2, which is implicated in all critical endothelial functions including proliferation, migration, and vessel formation (Ferrara et al., 2003; Olsson et al., 2006; Shibuya, 2006).

Emerging from these observations was the rationale to target the VEGF/VEGFR2 signaling pathway as an anti-angiogenic strategy, a notion that has subsequently been supported by a wealth of preclinical data as well as clinical results (Crawford and Ferrara, 2008; Jain, 2008). However, more rigorous expression analyses recently have revealed the expression of VEGF receptors, specifically VEGFR2, on non-endothelial cells, including hematopoietic cells, megakaryocytes, pancreatic duct cells, pericytes, and even tumor cells of various origins (Dallas et al., 2007; Greenberg et al., 2008; Hamerlik et al., 2012; Matsumoto and Claesson-Welsh, 2001; Silva et al., 2011). This suggests that VEGF likely has additional effects on tumors besides promoting neovascularization.

VEGF Signaling in Tumor Cells

In this study we identified an autocrine VEGF/VEGFR2 loop in GBM cells that negatively affects MET activity through recruitment of the phosphatase PTP1B to a VEGFR2/MET heterocomplex. Indeed, evidence for cross-talk between VEGFR2 or MET and other receptor tyrosine kinases (RTKs) is growing. Most recently, VEGFR2 expression was identified on pericytes where it physically associates with and suppresses PDGFRβ signaling, consequently ablating pericyte coverage of nascent vascular sprouts (Greenberg et al., 2008). These results are analogous to our own, conveying VEGF/VEGFR2 as a negative regulator of other RTKs by blocking their activation through direct interaction.

Both MET and VEGFR2 have been found to interact with a variety of other co-receptors and surface molecules as well (Birchmeier et al., 2003; Koch et al., 2011; Li et al., 2008; Trusolino et al., 2010). Notably, VEGFR2 and MET are each able to associate with neuropilin-1 (NRP-1), a receptor for class 3 semaphorins that is thought to enhance signaling of these two RTKs (Hu et al., 2007; Soker et al., 1998). However, our results suggest that NRP-1 is not a co-receptor of the VEGFR2/MET complex, which might not be unexpected because the heterocomplex blocks MET signaling, but we cannot rule out the association of other co-receptors within this complex.

The aforementioned results suggest that VEGF levels act as a sensor for the vascular and tumor cell compartments in part by sending signals through VEGFR2 complexes on endothelial cells and at least two distinct VEGFR2/RTK heterocomplexes (i.e. VEGFR2/MET on tumor cells and VEGFR2/PDGRβ on pericytes). One can speculate that the distinct associations of VEGFR2 with other RTKs might reflect a level of regulation by which VEGF can positively or negatively signal in different cell types. While high levels of VEGF facilitate angiogenesis and thereby enable tumor cells to expand, low levels of VEGF lead to a reduction in tumor vessel growth and protection of remaining vessels and concomitantly promote signals for GBM cells to move away from these undesirable conditions.

Microenvironmental Regulation of MET Activity During Anti-VEGF Therapy

MET transcription is induced by the hypoxia-inducible factor HIF-1α in some tumor cells, including GBM (Eckerich et al., 2007; Pennacchietti et al., 2003) and MET expression was found to be upregulated in a subset of bevacizumab-treated patients (Rose and Aghi, 2010). Because reduction in vessel density causes low oxygen tension, it is conceivable that

increased MET activity in response to anti-VEGF therapy might be regulated by hypoxia. However, we observed MET activity primarily at the invasive edges of tumors which are not hypoxic, rather than within the tumor mass where low oxygen tension is more severe. We also observed that HIF1α-KO murine GBM were much more invasive than wild type tumors, concomitant with high P-MET in the invasive areas (Blouw et al., 2003; Du et al., 2008a). Hence, these results demonstrate that the invasive phenotype cannot be exclusively driven by inadequate oxygen or nutrient supply.

Although we observed VEGFR2/MET complexes in the absence of ligand, the heterodimers appeared to coalesce into larger clusters only upon co-stimulation with HGF and VEGF, suggesting that additional proteins might further associate with the complex in the presence of both ligands. Indeed, we found that VEGF enhanced the recruitment of PTP1B to the VEGFR2/MET complex, which upon HGF stimulation, facilitated MET dephosphorylation. In addition to directly dephosphorylating ligand-stimulated RTK substrates such as MET, VEGFR2, EGFR, insulin receptor, and PDGFR (Galic et al., 2005; Haj et al., 2003; Nakamura et al., 2008; Sangwan et al., 2008), PTP1B also regulates their endosomal trafficking and internalization into multivesicular bodies (Eden et al., 2010; Sangwan et al., 2011; Stuible and Tremblay, 2010). In the context of VEGF-driven suppression of MET activation, however, we observed no significant differences in MET endocytosis with VEGF treatment, suggesting that the principal role of PTP1B in this mechanism is to directly dephosphorylate MET. We found that MET was predominantly localized to early endosomes when cells were stimulated with HGF with or without VEGF. Because MET can continue to signal as it progresses along the endocytic pathway (Abella et al., 2005), VEGF-enhanced recruitment and activity of PTP1B may likely be important in maintaining suppression of P-MET in the endosomal compartments. Accordingly, lowering VEGF levels and/or increasing HGF levels would lead to rapid MET reactivation and enhanced tumor cell invasiveness.

VEGF Regulates HGF-induced EMT-like Traits in GBM cells

Interestingly, activation of MET by genetic and pharmacologic VEGF inhibition increased invasion concomitant with induction of mesenchymal features. Similar to a recent report that MET signaling induces Snail (Grotegut et al., 2006), we observed Snail and N-Cadherin upregulation in GBM cells, which was surprisingly associated with T-cadherin downregulation. The latter observation implies an alternative cadherin switch distinct from the classical E-cadherin to N-cadherin switch in epithelial cells (Kalluri and Weinberg, 2009). T-cadherin is an atypical member of the cadherin family devoid of a transmembrane domain but anchored to the surface of the plasma membrane via a glycosylphosphatidylinositol anchor (Andreeva and Kutuzov, 2010). While it is expressed in many tumor vessels, downregulation of T-cadherin is observed in a variety of cancer cells and associated with a poorer prognosis (Andreeva and Kutuzov, 2010). In GBM cells, overexpression of T-cadherin suppresses proliferation and migration (Huang et al., 2003), consistent with our observation that T-cadherin expression was higher in circumscribed, minimally invasive VEGFKO-shMET GBM but absent in invasive GBM with high MET activity. In addition we found that HGF stimulation suppressed T-cadherin within 6 hours, suggesting that HGF-induced EMT signals affect T-cadherin transcription. Further

supporting a role for T-cadherin in an EMT-like acquisition in GBM is a recent report demonstrating that Zeb-1 suppresses T-cadherin and increases invasion in gallbladder cancer (Adachi et al., 2009).

Clinical Implication

These studies together suggest that one might be able to select GBM patients upfront who may likely develop a pro-invasive recurrence during bevacizumab treatment by evaluating MET and VEGFR2 expression in the tumor. This is particularly instrumental in light of the fact that GBM are heterogeneous by nature and can be classified into four distinct molecular subtypes (Phillips et al., 2006; Verhaak et al., 2010). Moreover, our results suggest that patients whose GBM are positive for both MET and VEGFR2 might benefit from treatment modalities that block both VEGF and HGF signaling. As we found VEGFR2 and MET expression on various tumor cell types besides GBM, combined VEGF and MET inhibition might also be useful in other cancer types as recently shown (Sennino et al., 2012). Finally, although HGF/MET is a major signaling node in promoting invasion, it is likely that other pro-invasive circuits are also involved in GBM invasion during the course of anti-VEGF therapy, or induced when MET is blocked. It will be important to elucidate whether these pathways are also linked to VEGF.

Experimental Procedures

Cell Culture and Reagents

Generation of murine WT-GBM and VEGFKO GBM has been previously described (Blouw et al., 2003). NSCGs were isolated from high-grade murine gliomas generated by transplantation of adult *Ink4/Arf*$^{-/-}$ neural stem cells expressing a constitutively active mutant of human EGFR, EGFRvIII (Phillips et al., 2012). Human GBM43 cells, which are primary cell cultures of patient-derived GBM specimens serially passaged as subcutaneous tumors in mice, have been previously described (Sarkaria et al., 2006). The primary human GBM cultures SF7996 and SF8161 were derived from freshly resected tumor specimens and expanded as glioma neural stem cell lines (Pollard et al., 2009). HEK293T fibroblast and BV-2 microglial cells were purchased from the American Type Culture Collection. HMEC cells have been previously described (Ades et al., 1992; Song et al., 2005). Overexpression and knockdown constructs are described in Supplemental Experimental Procedures.

Human GBM Specimens

We analyzed paired sets of surgical specimens from 10 patients with recurrent glioblastoma treated with bevacizumab at the University of California, San Francisco (UCSF), who demonstrated initial response but recurred while on therapy. Formalin-fixed and paraffin-embedded tumor specimens were collected during surgery from consenting patients, assigned a de-identifying number, and provided by the UCSF Brain Tumor Research Center Tissue Bank according to a protocol approved by the UCSF Committee on Human Research. Patients were selected based on availability of paired tumor specimens from recurrent tumor before and after bevacizumab treatment. Immunohistochemistry on human tissues was performed as described in Supplemental Experimental Procedures.

Animal Studies

Six- to eight-week old FvBN Rag1ko mice were intracranially implanted with 2.5 ml of 1×10^5 murine WT-GBM, VEGFKO, VEGFKO-VEGF, VEGFKO-scramble, VEGFKO-shMET1 or 2, NSCG, NSCG-VEGF, or human GBM43 tumor cells as described previously (Blouw et al., 2003; Du et al., 2008a). Mice bearing WT-GBMs were treated with 5 mg/kg B20 (kindly provided by Genentech, South San Francisco, CA) in PBS twice weekly by intraperitoneal injection beginning 3 days after tumor implantation until moribund. Sunitinib was administered to WT-GBM bearing mice at 40mg/kg daily by oral gavage starting 4 days after tumor injection until moribund. Mice were sacrificed when they developed side effects of tumor burden, such as weight loss and lateral recumbency, or at predefined time points for comparative analysis. Tumors were isolated from the brain and prepared for immunohistochemical staining, flow cytometric analyses, or protein and RNA isolation as described in Supplemental Experimental Procedures. All experiments involving animals in this study were reviewed and approved by the Institutional Animal Care and Use Committee at UCSF.

For further experimental details, see Supplemental Experimental Procedures.

Supplementary Material

Refer to Web version on PubMed Central for supplementary material.

Acknowledgments

We thank Dr. Veena Sangwan for PTP1B siRNA, Bina Kaplan for technical assistance, Dr. Zena Werb for MF1, and Drs. Zena Werb, William Weiss, and Susan Chang for thoughtful discussion. This work was supported by grants from the NIH (RO1CA099948; RO1CA113382 and U54CA163155 to G.B.) and the Canadian Institutes of Health Research (CTP-79857 to M.P.) K.V.L. was supported by a Leonard Heyman/American Brain Tumor Association Fellowship.

References

Abella JV, Peschard P, Naujokas MA, Lin T, Saucier C, Urbe S, Park M. Met/Hepatocyte growth factor receptor ubiquitination suppresses transformation and is required for Hrs phosphorylation. Mol. Cell. Biol. 2005; 25:9632–9645. [PubMed: 16227611]

Abounader R, Laterra J. Scatter factor/hepatocyte growth factor in brain tumor growth and angiogenesis. Neuro Oncol. 2005; 7:436–451. [PubMed: 16212809]

Adachi Y, Takeuchi T, Nagayama T, Ohtsuki Y, Furihata M. Zeb1-mediated T-cadherin repression increases the invasive potential of gallbladder cancer. FEBS Lett. 2009; 583:430–436. [PubMed: 19116147]

Ades EW, Candal FJ, Swerlick RA, George VG, Summers S, Bosse DC, Lawley TJ. HMEC-1: establishment of an immortalized human microvascular endothelial cell line. J. Invest. Dermatol. 1992; 99:683–690. [PubMed: 1361507]

Andreeva AV, Kutuzov MA. Cadherin 13 in cancer. Genes Chromosomes Cancer. 2010; 49:775–790. [PubMed: 20607704]

Bergers G, Hanahan D. Modes of resistance to anti-angiogenic therapy. Nat. Rev. Cancer. 2008; 8:592–603. [PubMed: 18650835]

Birchmeier C, Birchmeier W, Gherardi E, Vande Woude GF. Met, metastasis, motility and more. Nat. Rev. Mol. Cell Biol. 2003; 4:915–925. [PubMed: 14685170]

Blouw B, Song H, Tihan T, Bosze J, Ferrara N, Gerber HP, Johnson RS, Bergers G. The hypoxic response of tumors is dependent on their microenvironment. Cancer Cell. 2003; 4:133–146. [PubMed: 12957288]

Chamberlain MC. Radiographic patterns of relapse in glioblastoma. J. Neurooncol. 2011; 101:319–323. [PubMed: 21052776]

Crawford Y, Ferrara N. VEGF inhibition: insights from preclinical and clinical studies. Cell Tissue Res. 2008

Dallas NA, Fan F, Gray MJ, Van Buren G 2nd, Lim SJ, Xia L, Ellis LM. Functional significance of vascular endothelial growth factor receptors on gastrointestinal cancer cells. Cancer Metastasis Rev. 2007; 26:433–441. [PubMed: 17786539]

de Groot JF, Fuller G, Kumar AJ, Piao Y, Eterovic K, Ji Y, Conrad CA. Tumor invasion after treatment of glioblastoma with bevacizumab: radiographic and pathologic correlation in humans and mice. Neuro Oncol. 2010; 12:233–242. [PubMed: 20167811]

Du R, Lu KV, Petritsch C, Liu P, Ganss R, Passegue E, Song H, Vandenberg S, Johnson RS, Werb Z, Bergers G. HIF1alpha Induces the Recruitment of Bone Marrow-Derived Vascular Modulatory Cells to Regulate Tumor Angiogenesis and Invasion. Cancer Cell. 2008a; 13:206–220. [PubMed: 18328425]

Du R, Petritsch C, Lu K, Liu P, Haller A, Ganss R, Song H, Vandenberg S, Bergers G. Matrix metalloproteinase-2 regulates vascular patterning and growth affecting tumor cell survival and invasion in GBM. Neuro Oncol. 2008b; 10:254–264. [PubMed: 18359864]

Eckerich C, Zapf S, Fillbrandt R, Loges S, Westphal M, Lamszus K. Hypoxia can induce c-Met expression in glioma cells and enhance SF/HGF-induced cell migration. Int. J. Cancer. 2007; 121:276–283. [PubMed: 17372907]

Eden ER, White IJ, Tsapara A, Futter CE. Membrane contacts between endosomes and ER provide sites for PTP1B-epidermal growth factor receptor interaction. Nat. Cell Biol. 2010; 12:267–272. [PubMed: 20118922]

Ferrara N. Role of vascular endothelial growth factor in regulation of physiological angiogenesis. Am. J. Physiol. Cell Physiol. 2001; 280:C1358–1366. [PubMed: 11350730]

Ferrara N, Gerber HP, LeCouter J. The biology of VEGF and its receptors. Nat. Med. 2003; 9:669–676. [PubMed: 12778165]

Friedman HS, Prados MD, Wen PY, Mikkelsen T, Schiff D, Abrey LE, Yung WK, Paleologos N, Nicholas MK, Jensen R, et al. Bevacizumab alone and in combination with irinotecan in recurrent glioblastoma. J. Clin. Oncol. 2009; 27:4733–4740. [PubMed: 19720927]

Furnari FB, Fenton T, Bachoo RM, Mukasa A, Stommel JM, Stegh A, Hahn WC, Ligon KL, Louis DN, Brennan C, et al. Malignant astrocytic glioma: genetics, biology, and paths to treatment. Genes Dev. 2007; 21:2683–2710. [PubMed: 17974913]

Galic S, Hauser C, Kahn BB, Haj FG, Neel BG, Tonks NK, Tiganis T. Coordinated regulation of insulin signaling by the protein tyrosine phosphatases PTP1B and TCPTP. Mol. Cell. Biol. 2005; 25:819–829. [PubMed: 15632081]

Gandino L, Longati P, Medico E, Prat M, Comoglio PM. Phosphorylation of serine 985 negatively regulates the hepatocyte growth factor receptor kinase. J. Biol. Chem. 1994; 269:1815–1820. [PubMed: 8294430]

Greenberg JI, Shields DJ, Barillas SG, Acevedo LM, Murphy E, Huang J, Scheppke L, Stockmann C, Johnson RS, Angle N, Cheresh DA. A role for VEGF as a negative regulator of pericyte function and vessel maturation. Nature. 2008; 456:809–813. [PubMed: 18997771]

Grotegut S, von Schweinitz D, Christofori G, Lehembre F. Hepatocyte growth factor induces cell scattering through MAPK/Egr-1-mediated upregulation of Snail. EMBO J. 2006; 25:3534–3545. [PubMed: 16858414]

Haj FG, Markova B, Klaman LD, Bohmer FD, Neel BG. Regulation of receptor tyrosine kinase signaling by protein tyrosine phosphatase-1B. J. Biol. Chem. 2003; 278:739–744. [PubMed: 12424235]

Hamerlik P, Lathia JD, Rasmussen R, Wu Q, Bartkova J, Lee M, Moudry P, Bartek J Jr. Fischer W, Lukas J, et al. Autocrine VEGF-VEGFR2-Neuropilin-1 signaling promotes glioma stem-like cell viability and tumor growth. J. Exp. Med. 2012; 209:507–520. [PubMed: 22393126]

Hammond DE, Carter S, McCullough J, Urbe S, Vande Woude G, Clague MJ. Endosomal dynamics of Met determine signaling output. Mol. Biol. Cell. 2003; 14:1346–1354. [PubMed: 12686592]

Hu B, Guo P, Bar-Joseph I, Imanishi Y, Jarzynka MJ, Bogler O, Mikkelsen T, Hirose T, Nishikawa R, Cheng SY. Neuropilin-1 promotes human glioma progression through potentiating the activity of the HGF/SF autocrine pathway. Oncogene. 2007; 26:5577–5586. [PubMed: 17369861]

Huang ZY, Wu Y, Hedrick N, Gutmann DH. T-cadherin-mediated cell growth regulation involves G2 phase arrest and requires p21(CIP1/WAF1) expression. Mol. Cell. Biol. 2003; 23:566–578. [PubMed: 12509455]

Iwamoto FM, Abrey LE, Beal K, Gutin PH, Rosenblum MK, Reuter VE, DeAngelis LM, Lassman AB. Patterns of relapse and prognosis after bevacizumab failure in recurrent glioblastoma. Neurology. 2009; 73:1200–1206. [PubMed: 19822869]

Jain RK. Lessons from multidisciplinary translational trials on anti-angiogenic therapy of cancer. Nat. Rev. Cancer. 2008

Kalluri R, Weinberg RA. The basics of epithelial-mesenchymal transition. J. Clin. Invest. 2009; 119:1420–1428. [PubMed: 19487818]

Koch S, Tugues S, Li X, Gualandi L, Claesson-Welsh L. Signal transduction by vascular endothelial growth factor receptors. Biochem. J. 2011; 437:169–183. [PubMed: 21711246]

Koochekpour S, Jeffers M, Rulong S, Taylor G, Klineberg E, Hudson EA, Resau JH, Vande Woude GF. Met and hepatocyte growth factor/scatter factor expression in human gliomas. Cancer Res. 1997; 57:5391–5398. [PubMed: 9393765]

Kunkel P, Ulbricht U, Bohlen P, Brockmann MA, Fillbrandt R, Stavrou D, Westphal M, Lamszus K. Inhibition of glioma angiogenesis and growth in vivo by systemic treatment with a monoclonal antibody against vascular endothelial growth factor receptor-2. Cancer Res. 2001; 61:6624–6628. [PubMed: 11559524]

Lamszus K, Schmidt NO, Jin L, Laterra J, Zagzag D, Way D, Witte M, Weinand M, Goldberg ID, Westphal M, Rosen EM. Scatter factor promotes motility of human glioma and neuromicrovascular endothelial cells. Int. J. Cancer. 1998; 75:19–28. [PubMed: 9426685]

Lesslie DP, Summy JM, Parikh NU, Fan F, Trevino JG, Sawyer TK, Metcalf CA, Shakespeare WC, Hicklin DJ, Ellis LM, Gallick GE. Vascular endothelial growth factor receptor-1 mediates migration of human colorectal carcinoma cells by activation of Src family kinases. Br. J. Cancer. 2006; 94:1710–1717. [PubMed: 16685275]

Li X, Claesson-Welsh L, Shibuya M. VEGF receptor signal transduction. Methods Enzymol. 2008; 443:261–284. [PubMed: 18772020]

Liang WC, Wu X, Peale FV, Lee CV, Meng YG, Gutierrez J, Fu L, Malik AK, Gerber HP, Ferrara N, Fuh G. Cross-species vascular endothelial growth factor (VEGF)-blocking antibodies completely inhibit the growth of human tumor xenografts and measure the contribution of stromal VEGF. J. Biol. Chem. 2006; 281:951–961. [PubMed: 16278208]

Matsumoto T, Claesson-Welsh L. VEGF receptor signal transduction. Sci STKE. 2001; 2001:re21. [PubMed: 11741095]

Nakamura Y, Patrushev N, Inomata H, Mehta D, Urao N, Kim HW, Razvi M, Kini V, Mahadev K, Goldstein BJ, et al. Role of protein tyrosine phosphatase 1B in vascular endothelial growth factor signaling and cell-cell adhesions in endothelial cells. Circ. Res. 2008; 102:1182–1191. [PubMed: 18451337]

Olsson AK, Dimberg A, Kreuger J, Claesson-Welsh L. VEGF receptor signalling - in control of vascular function. Nat. Rev. Mol. Cell Biol. 2006; 7:359–371. [PubMed: 16633338]

Paez-Ribes M, Allen E, Hudock J, Takeda T, Okuyama H, Vinals F, Inoue M, Bergers G, Hanahan D, Casanovas O. Antiangiogenic therapy elicits malignant progression of tumors to increased local invasion and distant metastasis. Cancer Cell. 2009; 15:220–231. [PubMed: 19249680]

Pennacchietti S, Michieli P, Galluzzo M, Mazzone M, Giordano S, Comoglio PM. Hypoxia promotes invasive growth by transcriptional activation of the met protooncogene. Cancer Cell. 2003; 3:347–361. [PubMed: 12726861]

Phillips HS, Kharbanda S, Chen R, Forrest WF, Soriano RH, Wu TD, Misra A, Nigro JM, Colman H, Soroceanu L, et al. Molecular subclasses of high-grade glioma predict prognosis, delineate a

pattern of disease progression, and resemble stages in neurogenesis. Cancer Cell. 2006; 9:157–173. [PubMed: 16530701]

Phillips JJ, Huillard E, Robinson AE, Ward A, Lum DH, Polley MY, Rosen SD, Rowitch DH, Werb Z. Heparan sulfate sulfatase SULF2 regulates PDGFRalpha signaling and growth in human and mouse malignant glioma. J. Clin. Invest. 2012; 122:911–922. [PubMed: 22293178]

Pollard SM, Yoshikawa K, Clarke ID, Danovi D, Stricker S, Russell R, Bayani J, Head R, Lee M, Bernstein M, et al. Glioma stem cell lines expanded in adherent culture have tumor-specific phenotypes and are suitable for chemical and genetic screens. Cell Stem Cell. 2009; 4:568–580. [PubMed: 19497285]

Rong S, Bodescot M, Blair D, Dunn J, Nakamura T, Mizuno K, Park M, Chan A, Aaronson S, Vande Woude GF. Tumorigenicity of the met proto-oncogene and the gene for hepatocyte growth factor. Mol. Cell. Biol. 1992; 12:5152–5158. [PubMed: 1406687]

Rose SD, Aghi MK. Mechanisms of evasion to antiangiogenic therapy in glioblastoma. Clin. Neurosurg. 2010; 57:123–128. [PubMed: 21280504]

Rubenstein JL, Kim J, Ozawa T, Zhang M, Westphal M, Deen DF, Shuman MA. Anti-VEGF antibody treatment of glioblastoma prolongs survival but results in increased vascular cooption. Neoplasia. 2000; 2:306–314. [PubMed: 11005565]

Sangwan V, Abella J, Lai A, Bertos N, Stuible M, Tremblay ML, Park M. Protein-tyrosine phosphatase 1B modulates early endosome fusion and trafficking of Met and epidermal growth factor receptors. J. Biol. Chem. 2011; 286:45000–45013. [PubMed: 22045810]

Sangwan V, Paliouras GN, Abella JV, Dube N, Monast A, Tremblay ML, Park M. Regulation of the Met receptor-tyrosine kinase by the protein-tyrosine phosphatase 1B and T-cell phosphatase. J. Biol. Chem. 2008; 283:34374–34383. [PubMed: 18819921]

Sarkaria JN, Carlson BL, Schroeder MA, Grogan P, Brown PD, Giannini C, Ballman KV, Kitange GJ, Guha A, Pandita A, James CD. Use of an orthotopic xenograft model for assessing the effect of epidermal growth factor receptor amplification on glioblastoma radiation response. Clin. Cancer. Res. 2006; 12:2264–2271. [PubMed: 16609043]

Sennino B, Ishiguro-Oonuma T, Wei Y, Naylor RM, Williamson CW, Bhagwandin V, Tabruyn SP, You W-K, Chapman HA, Christensen JG, et al. Suppression of Tumor Invasion and Metastasis by Concurrent Inhibition of c-Met and VEGF Signaling in Pancreatic Neuroendocrine Tumors. Cancer Discovery. 2012; 2:270–287. [PubMed: 22585997]

Shibuya M. Differential roles of vascular endothelial growth factor receptor-1 and receptor-2 in angiogenesis. J Biochem Mol Biol. 2006; 39:469–478. [PubMed: 17002866]

Silva SR, Bowen KA, Rychahou PG, Jackson LN, Weiss HL, Lee EY, Townsend CM Jr. Evers BM. VEGFR-2 expression in carcinoid cancer cells and its role in tumor growth and metastasis. Int. J. Cancer. 2011; 128:1045–1056. [PubMed: 20473929]

Soderberg O, Leuchowius KJ, Gullberg M, Jarvius M, Weibrecht I, Larsson LG, Landegren U. Characterizing proteins and their interactions in cells and tissues using the in situ proximity ligation assay. Methods. 2008; 45:227–232. [PubMed: 18620061]

Soker S, Takashima S, Miao HQ, Neufeld G, Klagsbrun M. Neuropilin-1 is expressed by endothelial and tumor cells as an isoform-specific receptor for vascular endothelial growth factor. Cell. 1998; 92:735–745. [PubMed: 9529250]

Song S, Ewald AJ, Stallcup W, Werb Z, Bergers G. PDGFRbeta+ perivascular progenitor cells in tumours regulate pericyte differentiation and vascular survival. Nat. Cell Biol. 2005; 7:870–879. [PubMed: 16113679]

Spannuth WA, Nick AM, Jennings NB, Armaiz-Pena GN, Mangala LS, Danes CG, Lin YG, Merritt WM, Thaker PH, Kamat AA, et al. Functional significance of VEGFR-2 on ovarian cancer cells. Int. J. Cancer. 2009; 124:1045–1053. [PubMed: 19058181]

Stenmark H. Rab GTPases as coordinators of vesicle traffic. Nat. Rev. Mol. Cell Biol. 2009; 10:513–525. [PubMed: 19603039]

Stuible M, Tremblay ML. In control at the ER: PTP1B and the down-regulation of RTKs by dephosphorylation and endocytosis. Trends Cell Biol. 2010; 20:672–679. [PubMed: 20864346]

Sundberg C, Nagy JA, Brown LF, Feng D, Eckelhoefer IA, Manseau EJ, Dvorak AM, Dvorak HF. Glomeruloid microvascular proliferation follows adenoviral vascular permeability factor/vascular

endothelial growth factor-164 gene delivery. Am. J. Pathol. 2001; 158:1145–1160. [PubMed: 11238063]

Thiery JP, Acloque H, Huang RY, Nieto MA. Epithelial-mesenchymal transitions in development and disease. Cell. 2009; 139:871–890. [PubMed: 19945376]

Trusolino L, Bertotti A, Comoglio PM. MET signalling: principles and functions in development, organ regeneration and cancer. Nat. Rev. Mol. Cell Biol. 2010; 11:834–848. [PubMed: 21102609]

Tso CL, Shintaku P, Chen J, Liu Q, Liu J, Chen Z, Yoshimoto K, Mischel PS, Cloughesy TF, Liau LM, Nelson SF. Primary glioblastomas express mesenchymal stem-like properties. Mol. Cancer Res. 2006; 4:607–619. [PubMed: 16966431]

van Bruggen N, Thibodeaux H, Palmer JT, Lee WP, Fu L, Cairns B, Tumas D, Gerlai R, Williams SP, van Lookeren Campagne M, Ferrara N. VEGF antagonism reduces edema formation and tissue damage after ischemia/reperfusion injury in the mouse brain. J. Clin. Invest. 1999; 104:1613–1620. [PubMed: 10587525]

Verhaak RG, Hoadley KA, Purdom E, Wang V, Qi Y, Wilkerson MD, Miller CR, Ding L, Golub T, Mesirov JP, et al. Integrated genomic analysis identifies clinically relevant subtypes of glioblastoma characterized by abnormalities in PDGFRA, IDH1, EGFR, and NF1. Cancer Cell. 2010; 17:98–110. [PubMed: 20129251]

Vredenburgh JJ, Desjardins A, Herndon JE 2nd, Dowell JM, Reardon DA, Quinn JA, Rich JN, Sathornsumetee S, Gururangan S, Wagner M, et al. Phase II trial of bevacizumab and irinotecan in recurrent malignant glioma. Clin. Cancer. Res. 2007; 13:1253–1259. [PubMed: 17317837]

Wang R, Chadalavada K, Wilshire J, Kowalik U, Hovinga KE, Geber A, Fligelman B, Leversha M, Brennan C, Tabar V. Glioblastoma stem-like cells give rise to tumour endothelium. Nature. 2010; 468:829–833. [PubMed: 21102433]

Wang R, Ferrell LD, Faouzi S, Maher JJ, Bishop JM. Activation of the Met receptor by cell attachment induces and sustains hepatocellular carcinomas in transgenic mice. J. Cell Biol. 2001; 153:1023–1034. [PubMed: 11381087]

Wick W, Wick A, Weiler M, Weller M. Patterns of progression in malignant glioma following anti-VEGF therapy: perceptions and evidence. Curr Neurol Neurosci Rep. 2011; 11:305–312. [PubMed: 21279815]

Highlights

VEGF blocks HGF-induced tumor invasion by recruiting PTP1B to a MET/VEGFR2 complex

VEGF inhibition enhances MET activity, mesenchymal transformation and invasion in GBM

Combined VEGF and MET inhibition blocks invasion and prolongs survival in GBM

Significance

Bevacizumab has been approved for the treatment of GBM patients with recurrent disease and is currently being evaluated for frontline therapy. Most patients initially experience beneficial effects from the treatment but all invariably confront tumor regrowth. About 20-30% of recurrent tumors elicit an infiltrating and more diffuse growth pattern that renders surgical resection unfeasible and imparts detrimental effects. The ability to identify GBM patients who will benefit from anti-angiogenic treatment without developing more invasive tumors is therefore pivotal. Here we provide the molecular mechanisms by which VEGF ablation causes enhanced invasion. These findings support combined treatment strategies targeting both VEGF and MET in GBM patients to overcome pro-invasive resistance and prolong survival.

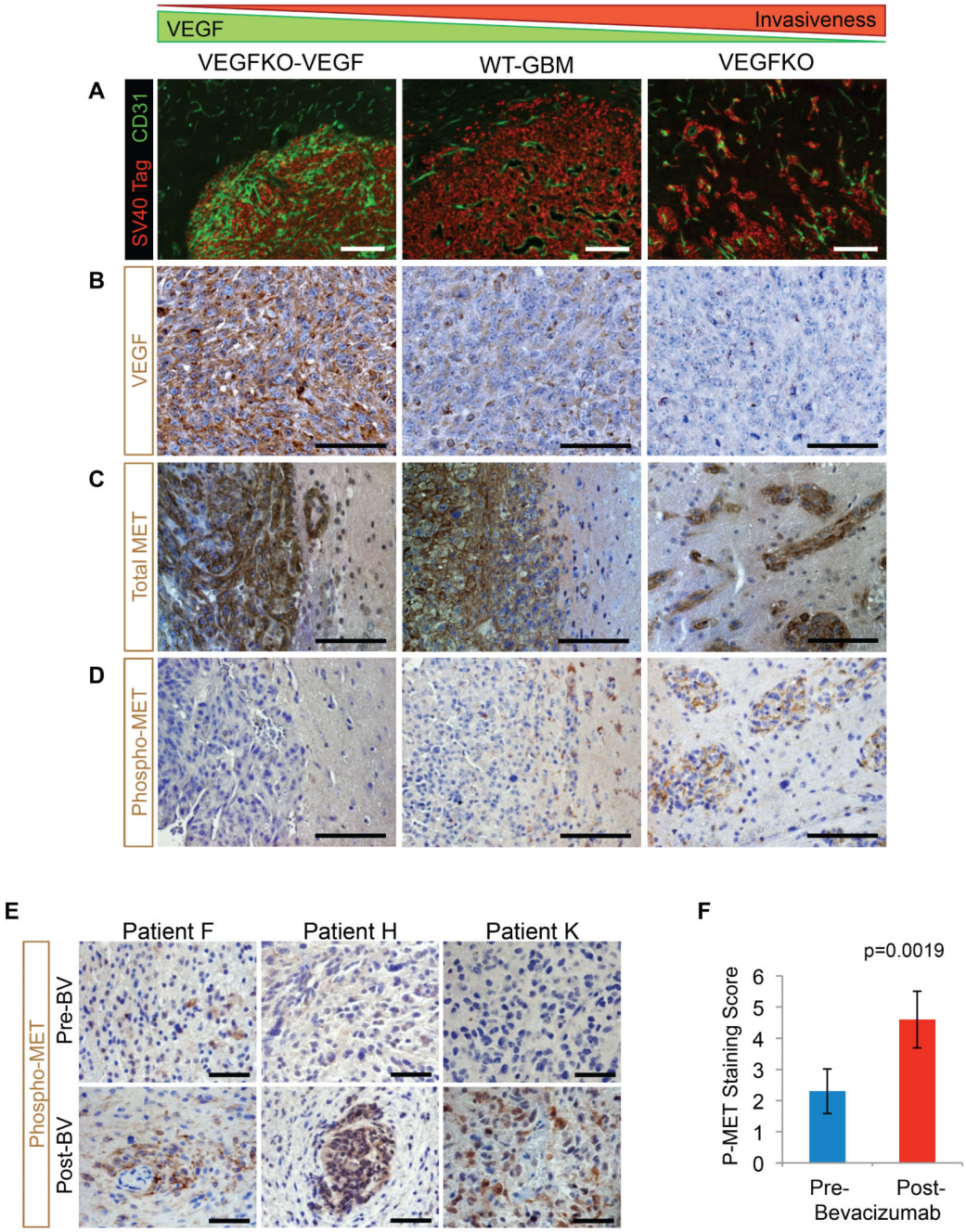

Figure 1. VEGF Expression is Inversely Correlated with Perivascular Invasion and MET Phosphorylation

(A) Tumors from intracranial implantion of indicated murine GBM cells were fluorescently stained for SV40 Large T-Antigen and CD31 to detect tumor cells and vasculature, respectively. Scale bars, 200 μm.

(B-D) IHC staining for VEGF (B), total MET (C), and phospho-MET (D) in orthotopic murine GBM. Scale bars, 100 μm.

(E) IHC staining for phospho-MET in paired human GBM surgical specimens before and after bevacizumab (BV) treatment. Scale bars, 50 μm.

(F) P-MET staining score (mean±SEM) of 10 human GBM before and after bevacizumab treatment based on a composite score as described in Supplemental Experimental Procedures.

See also Figure S1.

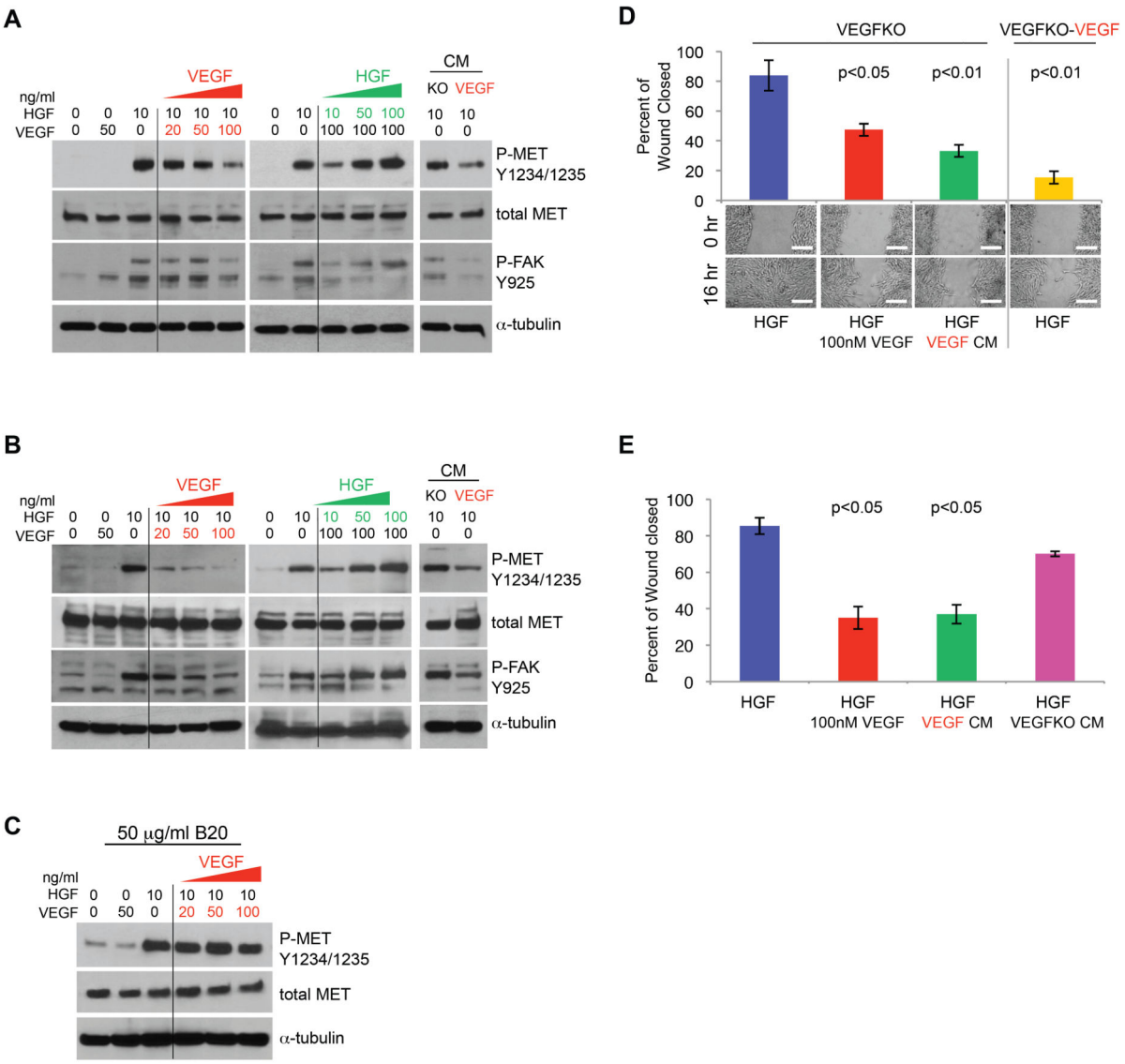

Figure 2. VEGF Suppresses HGF-stimulated MET Phosphorylation and Cell Motility

(A) Western blot analysis of cell lysates from murine VEGFKO cells stimulated with various concentrations of HGF and/or VEGF for P-MET, total MET, and P-FAK. VEGFKO cells were also incubated with their own (KO) or VEGFKO-VEGF cells (VEGF) conditioned media (CM). α-tubulin was used for loading control.

(B) Western blot analysis of human primary GBM43 cells treated with HGF and/or VEGF for P-MET, total MET, P-FAK, and α-tubulin.

(C) Western blot analysis of human GBM43 cells treated with B20 and stimulated with HGF and/or VEGF.

(D) Wound-healing assay of HGF-stimulated VEGFKO cells or VEGFKO-VEGF cells. VEGFKO cells were treated with either exogenous VEGF or CM from VEGFKO-VEGF cells (VEGF CM). Top, quantification of wound closure (mean±SEM). p-values compared

to VEGFKO cells stimulated with HGF only. Bottom, representative images of wounded cell monolayers. Scale bars, 150μm.

(E) Wound-healing assay of GBM43 cells treated with exogenous VEGF, VEGF CM, and VEGFKO CM (mean±SEM). p-values compared to GBM43 cells stimulated with HGF only.

See also Figure S2.

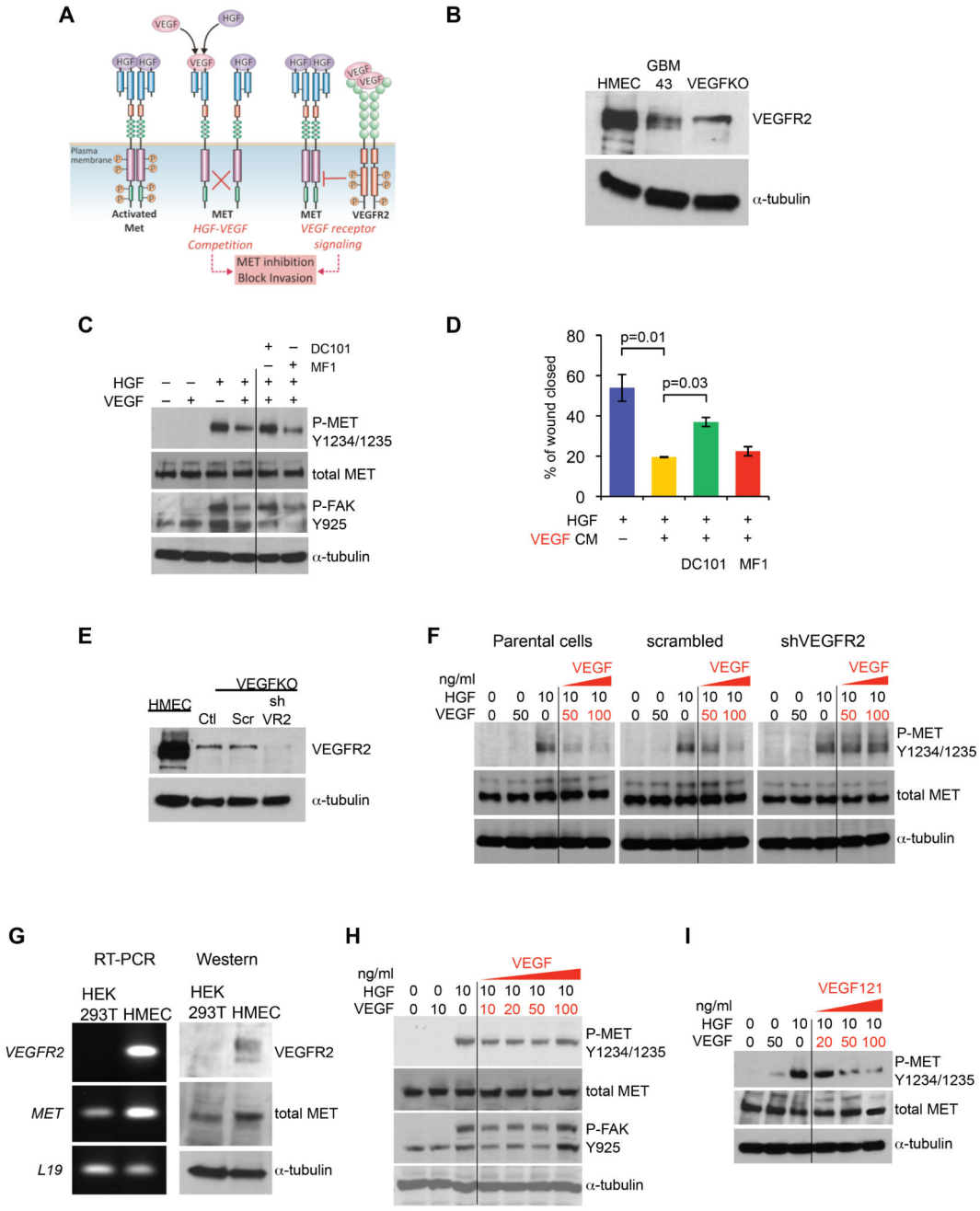

Figure 3. VEGFR2 is Required for VEGF to Suppress HGF-stimulated MET Phosphorylation and Cell Motility

(A) Schematic of possible ways by which VEGF can block MET activation.

(B) Western blot analysis detecting relative VEGFR2 expression in GBM43 and VEGFKO tumor cells. Human microvascular endothelial cells (HMEC) were used as a positive control.

(C) VEGFKO cells stimulated with HGF or VEGF as indicated were treated with 100 μg/ml of DC101 or 100 μg/ml of MF1 and lysates subjected to immunoblotting.

(D) Motility of VEGFKO cells incubated with VEGF CM and treated with either 100 μg/ml DC101 or MF1 was assessed in the wound-healing assay (mean±SEM).
(E) Western blot analysis showing stable knockdown of VEGFR2 in VEGFKO cells transduced with VEGFR2 shRNA (shVR2). Parental control cells (Ctl) and a scrambled shRNA sequence (Scr) are also shown. HMEC were used as a positive control.
(F) Parental VEGFKO cells or VEGFKO cells transduced with scrambled shRNA or shRNA targeting VEGFR2 were stimulated with HGF and/or VEGF and subjected to immunoblotting as indicated.
(G) RT-PCR and western blot analyses for *VEGFR2* and *MET* expression in HEK293T fibroblasts. HMEC served as positive control for VEGFR2 expression. *L19* and α-tubulin were loading controls for RT-PCR and western blot, respectively.
(H) HEK293T cells stimulated with HGF and indicated concentrations of VEGF were subjected to western blot analysis as indicated.
(I) Western blot analysis of VEGFKO cells stimulated with HGF or VEGF121 as indicated.
See also Figure S3.

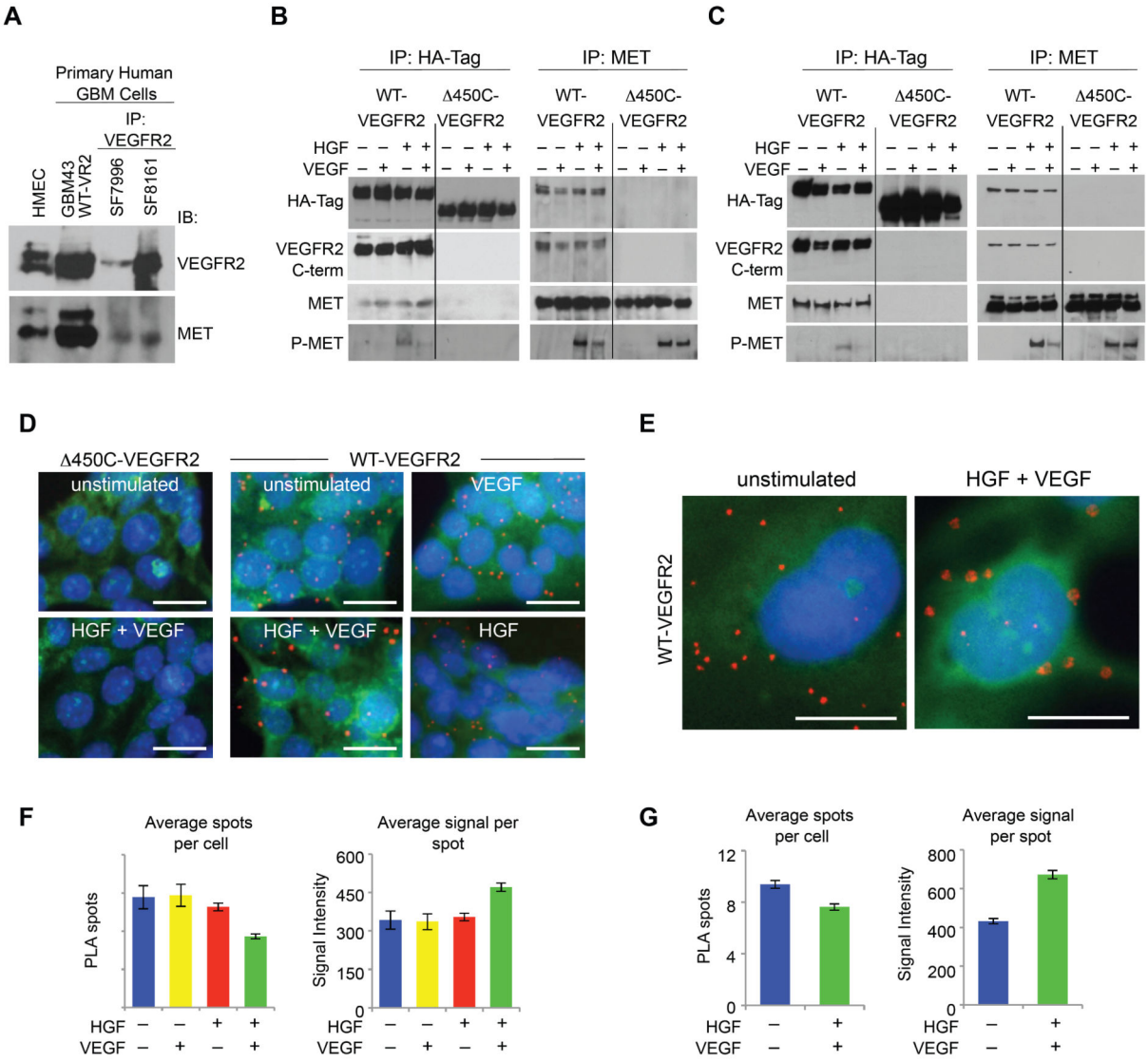

Figure 4. MET and VEGFR2 Associate in a Heterocomplex

(A) Co-immunoprecipitation (IP) of endogenous VEGFR and MET in two primary human GBM cultures (SF7796 and SF8161) as visualized by IP of VEGFR2 followed by immunoblotting for VEGFR2 and MET. Whole cell lysates from HMEC and human primary GBM43 cells overexpressing VEGFR2 by adenoviral transduction (GBM43 WT-VR2) were run alongside as positive controls.

(B-C) Murine VEGFKO cells (B) or GBM43 cells (C) transduced by adenovirus to overexpress HA-tagged WT-VEGFR2 or Δ450C-VEGFR2 with or without stimulation of HGF or VEGF as indicated were lysed and immunoprecipitated using indicated antibodies and the immunoprecipitates then immunoblotted as indicated.

(D-E) Representative images of PLA in murine VEGFKO (D) or human GBM43 (E) cells expressing WT-VEGFR2 or Δ450C-VEGFR2 after treatment with the indicated growth factors. Red spots are regions of signal amplification denoting VEGFR2 and MET

interaction. Cytoskeletal staining (FITC-phalloidin) is green, and nuclear stain (DAPI) is blue. Scale bars, 20 μm.

(F-G) Quantification of PLA signals in murine VEGFKO (F) and human GBM43 (G) cells transduced with WT-VEGFR2 (mean±SEM).

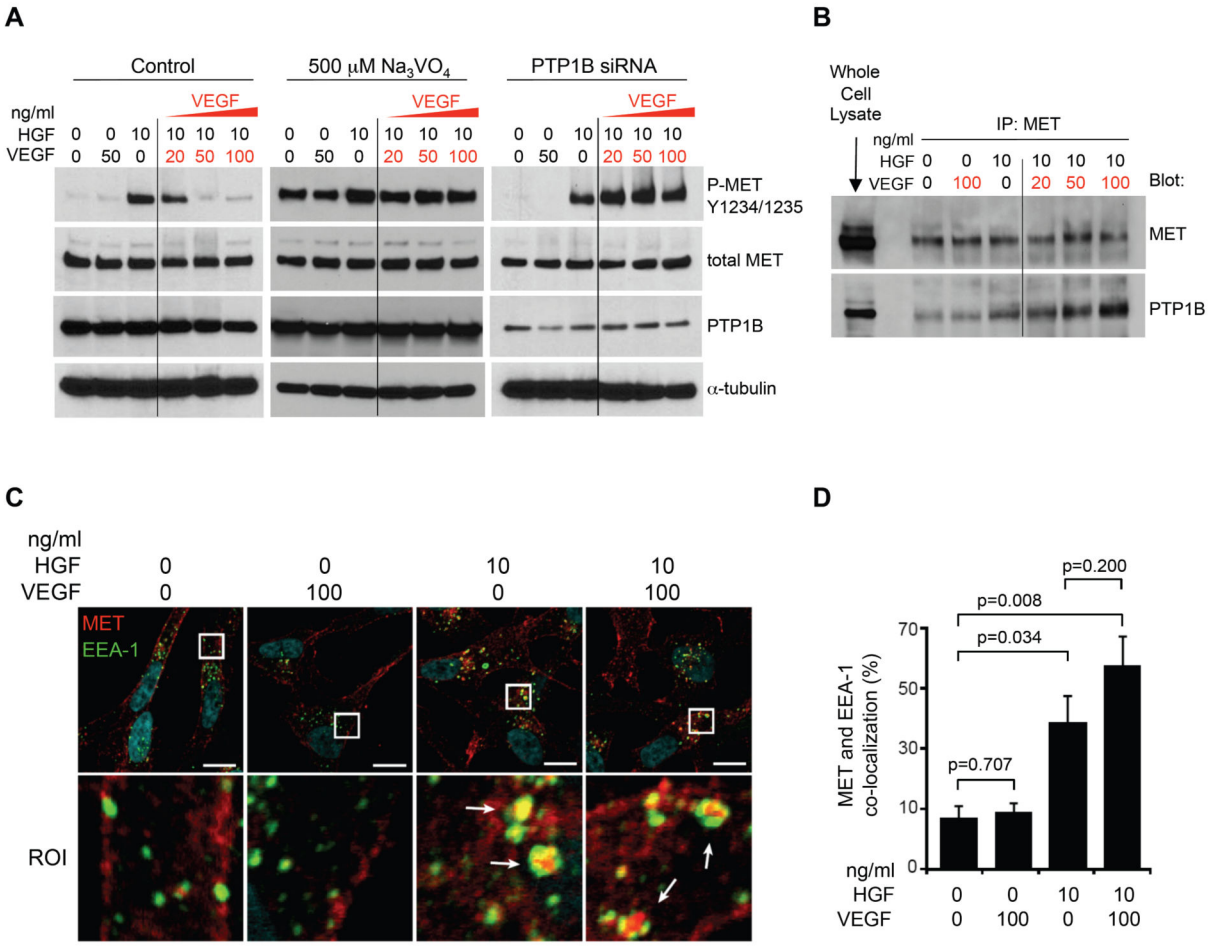

Figure 5. VEGF Signaling Increases PTP1B Recruitment to MET

(A) Control GBM43 cells, GBM43 cells treated with sodium orthovanadate (Na_3VO_4) for 30 min, or GBM43 cells transfected with PTP1B siRNA were stimulated with HGF, VEGF, or both ligands at the concentrations indicated and lysates analyzed by western blot for P-MET, total MET, and PTP1B.

(B) GBM43 cells stimulated with HGF and/or VEGF were crosslinked with the membrane-permeable and cleavable cross-linker DSP and 250 μg of each lysate immunoprecipitated with an anti-MET antibody, followed by immunoblotting for MET and PTP1B. GBM43 whole cell lysate served as a positive control for analysis of the immunoprecipitates.

(C) Representative images of immunofluorescent staining of GBM43 cells treated with HGF and/or VEGF for MET (red), EEA-1 (green), and DAPI (blue). ROI: higher magnification of the indicated area. Arrows indicate co-localization of MET and EEA-1-positive vesicles. Scale bar = 10 μm.

(D) Quantification of co-localization between MET and EEA-1 staining (mean±SEM).

See also Figure S4.

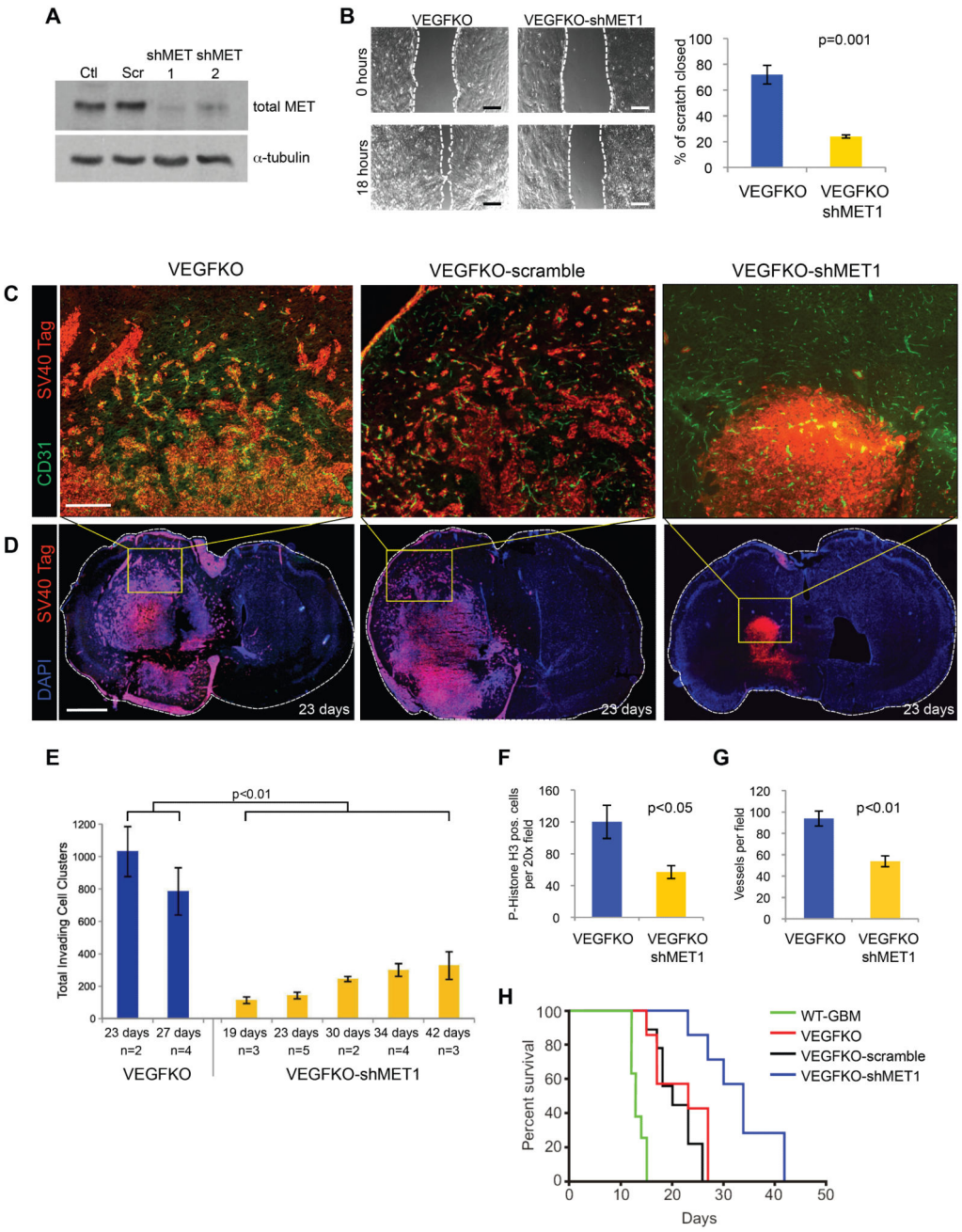

Figure 6. MET Knockdown Blocks Tumor Invasion and Promotes Survival of VEGF-deficient Tumors

(A) Immunoblot analysis of MET expression in VEGFKO cells stably transduced with two independent shRNAs targeting MET. Parental VEGFKO cells (Ctl) and VEGFKO cells transduced with a scrambled shRNA (Scr) are also shown.

(B) Representative images (left) and quantification (right, mean±SEM) of a wound-healing assay comparing migration of VEGFKO-shMET1 cells to VEGFKO cells. Dashed white lines indicate edge of wound. Scale bar, 100 μm.

(C-D) Immunohistochemical staining of intracranial VEGFKO, VEGFKO-scrambled, and VEGFKO-shMET1 tumors with SV40 large T-antigen (red) and CD31 (green) (C), or with SV40 large T-antigen (red) and DAPI (blue) (D), to visualize tumor cells and vasculature, respectively. Yellow boxes in (D) (scale bar, 1 mm) represent the region of magnification shown in (C) (scale bar, 200 μm). Images are representative of time-matched samples 23 days post-implantation.

(E) Quantification of total invasion from the primary tumor mass in VEGFKO or VEGFKO-shMET1 tumors over various time points (mean±SEM). The number of mice analyzed for each condition and time point is indicated.

(F-G) Proliferation (F) and vessel density (G) in orthotopic VEGFKO and VEGFKO-shMET1 tumors 23 days after tumor inoculation as determined by phospho-histone H3 and CD31 staining, respectively (mean±SEM).

(H) Kaplan-Meier survival curves of mice intracranially implanted with WT-GBM, VEGFKO, VEGFKO-scrambled, and VEGFKO-shMET1 cells. p=0.007 for VEGFKO-shMET1 vs. VEGFKO-scramble.

See also Figure S5.

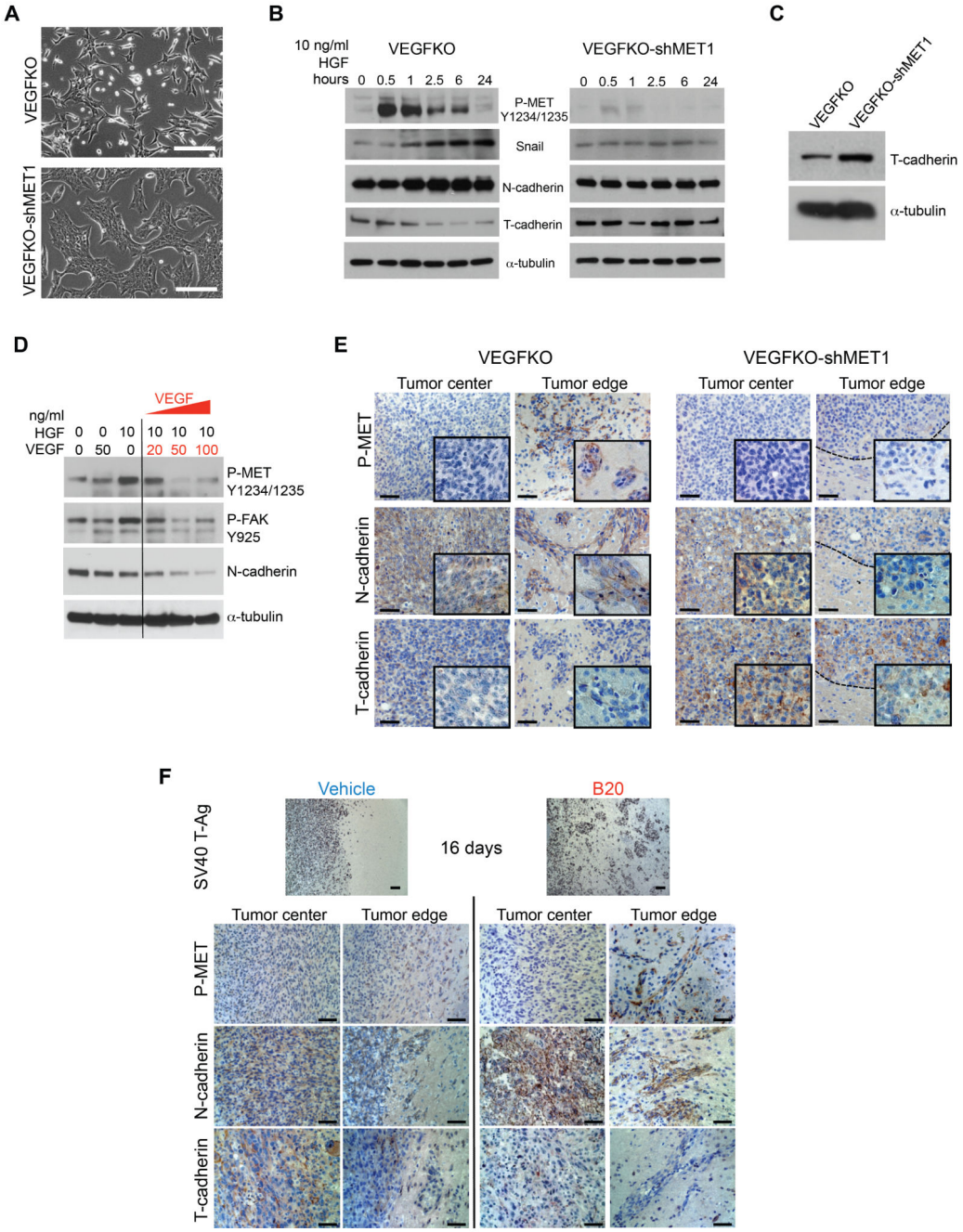

Figure 7. HGF/MET Signaling Induces an EMT-like Transition in GBM

(A) Representative phase contrast microscopy images of VEGFKO and VEGFKO-shMET1 cells. Scale bars, 100 μm.

(B) Immunoblot analysis of VEGFKO or VEGFKO-shMET1 cells stimulated with HGF for the indicated times for P-Met, Snail, N-cadherin, and T-cadherin expression.

(C) Immunoblot analysis of T-cadherin expression in VEGFKO-shMET1 cells and parental VEGFKO cells.

(D) Immunoblot analysis of VEGFKO cell lysates 6 hours after stimulation with HGF or indicated concentrations of VEGF.

(E-F) Immunohistochemical staining of intracranial mouse GBMs for P-MET, N-cadherin, and T-cadherin (brown). Sections were counterstained with hematoxylin (blue). Staining at the center of the main tumor mass or at the tumor rim is shown as indicated. (E) Representative images of time-matched (day 27) VEGFKO and VEGFKO-shMET1 tumors. Dashed lines indicate the smooth border of VEGFKO-shMET1 tumors. (F) Mice bearing orthotopic WT-GBM were treated with B20 or vehicle beginning 3 days after tumor implantation. Representative staining of tumors from mice sacrificed 16 days after tumor implantation are shown. Tumor cells were visualized by staining for SV40 Tag (top). Scale bars, 50 μm.

See also Figure S6.

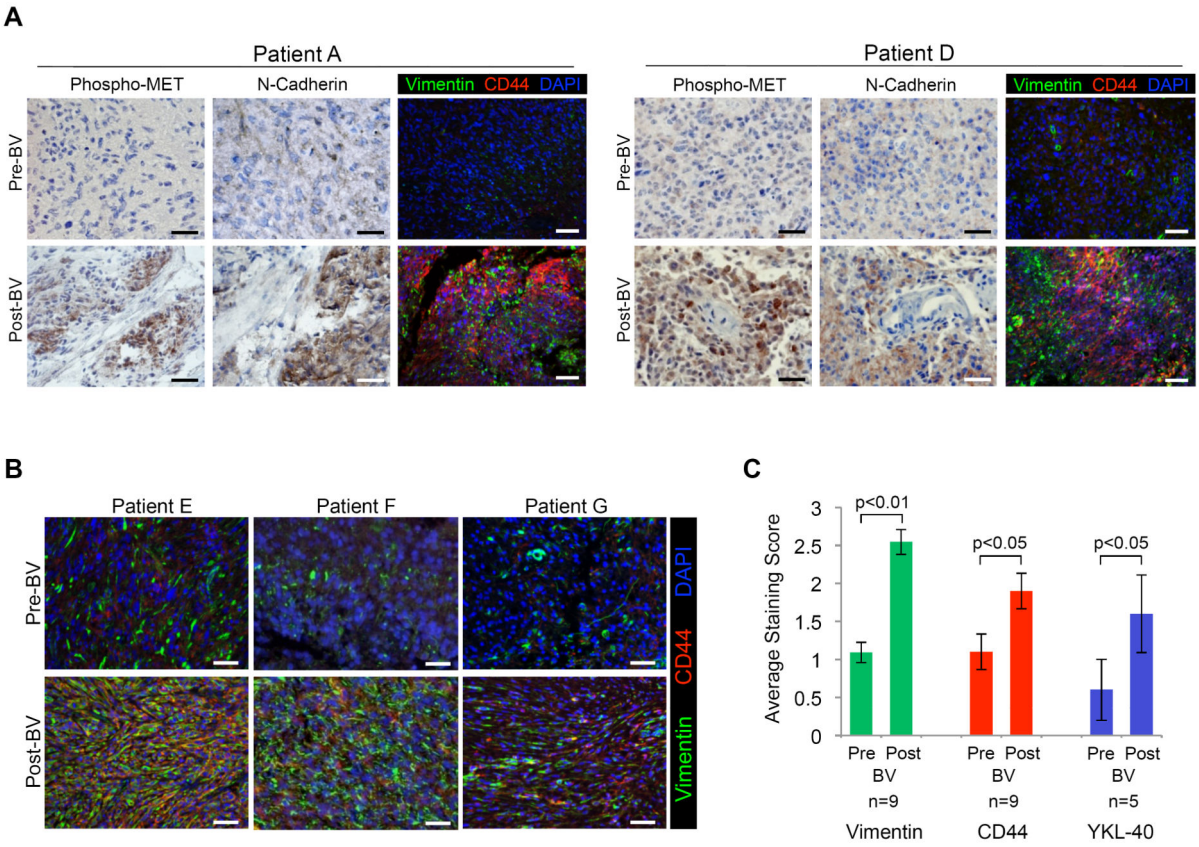

Figure 8. Bevacizumab-Resistant Human GBM Exhibit Increased P-MET and Expression of Mesenchymal Markers

(A-B) Paired human GBM samples obtained before and after treatment with bevacizumab (BV) were immunohistochemically stained for P-MET and N-cadherin (brown) and counterstained with hematoxylin (blue) (A). Representative images of staining from the same area of serial sections are shown. Tissues were also fluorescently co-stained for the mesenchymal markers vimentin (green) and CD44 (red) and nuclei visualized with DAPI (blue) (A-B). Scale bars, 50 μm.

(C) Staining scores (mean±SEM) of the mesenchymal markers vimentin, CD44, and YKL-40 in paired human GBM specimens before and after BV. Each sample was scored on a scale of 0-3 and the number of paired patient samples analyzed for marker indicated.